molecular pharmaceutics

Article

pubs.acs.org/molecularpharmaceutics

Molecular Structuring and Phase Transition of Lipid-Based Formulations upon Water Dispersion: A Coarse-Grained Molecular Dynamics Simulation Approach

Per Larsson,* Linda C. Alskär, and Christel A. S. Bergström

Department of Pharmacy, Uppsala University, Uppsala Biomedical Center, P.O. Box 580, SE-751 23 Uppsala, Sweden

Supporting Information

ABSTRACT: The internal molecular structure of lipid-based formulations (LBFs) is poorly understood. In this work we aimed at establishing coarse-grained molecular dynamics simulations as a tool for rapid screening and investigation of the internal environment of these formulations. In order to study complex LBFs composed of different kinds of lipids we simulated a number of systems containing either medium-chain or long-chain lipids with varying proportions of tri-, di-, and monoglycerides. Structural and dynamic measurements and analyses identified that the internal environment in a mixture of lipids was locally ordered even in the absence of water, which might explain some of the previously reported effects on drug solubility in these systems. Further, phase changes occurring upon water dispersion are well captured with coarse-grained simulations. Based on these simulations we conclude that the coarse-grained methodology is a promising in silico approach for rapid screening of structures formed in complex formulations. More importantly it facilitates molecular understanding of interactions between excipients and water at a feasible time scale and, hence, opens up for future virtual drug formulation studies.

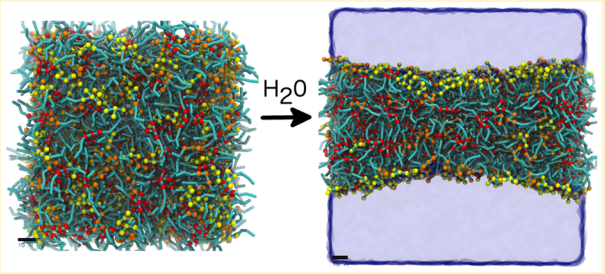

KEYWORDS: *lipid-based formulations, coarse-grained molecular dynamics, phase transition*

INTRODUCTION

Oral administration of drugs requires the active pharmaceutical ingredient (API) to be sufficiently soluble in gastric or intestinal fluid to allow complete absorption. For many compounds formulation strategies are required to increase the intestinal concentration and enable absorption. One such strategy is the use of lipid-based formulations (LBFs), which contain lipids, surfactants, and/or cosolvents. The solubility of the drug in the formulation is affected by each of the components. In 2006, Pouton established the lipid formulation classification system (LFCS) in which LBFs are classified according to their lipid content and performance upon dispersion and digestion.[1,2] This system has since been used to improve understanding of the behavior of formulated drugs. In particular, the system has been used to study LBF performance in intestinal fluids, in response to enzymatic digestion of, for example, LBF di- and triglycerides.

LBF design and performance has typically been assessed experimentally; however, the increased use of computational tools could improve our understanding of, e.g., drug loading of the formulation and performance after oral administration at a molecular level. One such tool involves molecular dynamics (MD) simulations. One benefit with MD simulations is that they can be performed to study LBFs before they are dispersed in water. It is difficult to characterize the internal structure of the dry LBF (i.e., all the formulation components prior to dispersion in water) using traditional experimental techniques.[3] Most classical scattering methods are not sensitive enough, although more sophisticated methods such as small-angle X-ray or neutron scattering could be useful.[4,5] MD simulation offers an alternative to these approaches and allows for a detailed understanding of many phenomena that are difficult or even impossible to probe experimentally. Specifically, for lipid−water interactions, a few examples include H-bond network forming at the membrane interface[6] and the influence of lipid bilayers on dynamics of water at the lipid bilayer surface.[7] To date, MD simulations have also been used to study phase behavior and to follow the fate of various drugs during dispersion of the LBF in water,[8] or digestion.[9,10] However, the latter studies are relatively few, mainly because MD simulations performed with a classical all-atom (AA) force field are computationally costly. As an alternative to AA simulations, it is possible to coarse-grain a molecular system on a number of levels.[11] The popular Martini force field,[12,13] for example, uses a mapping strategy involving the grouping of about four atoms into a single bead. This serves two primary purposes: it drastically reduces the number of particles in a particular system (for

Special Issue: Industry-Academic Collaboration in Oral Biopharmaceutics: The European IMI OrBiTo Project

Received: May 12, 2017
Revised: August 3, 2017
Accepted: August 11, 2017
Published: August 11, 2017

DOI: 10.1021/acs.molpharmaceut.7b00397
Mol. Pharmaceutics 2017, 14, 4145−4153

example, one Martini water bead corresponds to four individual water molecules), and it also speeds up the overall dynamics in the system, leading to faster transitions between substates in a simulation ensemble. It is possible to change the resolution scales, e.g., from the coarse-grained (CG) scale to the atomistic level, allowing the study of particularly interesting aspects at an atomic level. The Martini model has been used successfully in the past to study a number of lipid phase phenomena, such as formation of gel phases[14,15] and inverted hexagonal[16] and cubic phases.[17] While all CG methods to some extent suffer from reduced spatial and chemical resolution, many examples such as the ones discussed here show the general applicability of the Martini force field. For a more in-depth discussion of the strengths and weaknesses of the Martini model, we refer the reader to the comprehensive review by Marrink and Tieleman.[18]

A long-term goal for us is to better understand solubilization of drugs formulated as LBFs. We therefore decided to explore whether CG-based MD simulations could help us with this matter. For instance, it has been shown that the solubility of a drug in an LBF can be approximated by combining the solubility values of the drug in the individual constituents of the formulation, weighted by the mass ratio of each compound in the formulation.[2,19−21] To date, the molecular reasoning behind this has been unclear, but we are speculating that it is a result of nanostructuring of the dry LBF. If the excipients exist as "local clusters" in these nanostructures, each of the nanostructures would perform as the single excipient (with the drug solubilized either completely within these structures or at the interface with the surrounding environment), and, hence, the solubility of the drug in that local environment would be the same as in the excipient alone. Thus, in this paper, we focused on establishing CG MD simulations using the Martini force field as a tool for rapid screening of local nanostructuring of LFCS class 1 model LBFs consisting of different kinds of glycerides; we examined the dry form of the LBFs prior to dispersion in water to mimic the formulation in a capsule as well as LBFs dispersed in water to mimic the structures likely to form after intake of a lipid-filled capsule with a glass of water.

METHODS

System Preparation and Setup. We used the Martini CG force field to study LBFs with different compositions of medium- and long-chain tri-, di-, and monoglycerides. The CG molecular structures are shown in Figure S1, where the differences between the AA and CG representations are clarified. As with earlier work with AA-based formulations,[8] we performed a series of simulations at different water/lipid ratios from 0% (w/w), representing the dry formulation in the capsule, to 5, 10, 20, 50, and 75% water, representing the dispersed sample. Further, we mimic digestion by varying the lipid composition from only triglycerides over systems of mono-, di-, and triglycerides to systems only including monoglycerides. Table 1 contains an overview of all the explored systems.

The initial parameters used for the different lipids were taken from those published earlier by Vuorela et al.[22] and adapted to reflect different lengths of carbon chain and numbers of lipid tails. This model uses one C1 bead together with three Na beads for the glycerol headgroup, and C1 beads for the alkyl chains. All initial systems and topologies are available as Supporting Information.

Table 1. Summary of the Simulations Performed To Investigate the Structure of LBFs[a]

system	no. of triglycerides	no. of diglycerides	no. of monoglycerides
A	1200		
B	600	600	60
C	400	400	400
D		600	600
E			1200
F	1200		
G	600	600	
H	400	400	400
I		600	600
J			1200

[a]Systems A−E are representative of medium-chain lipid-based formulations containing lipids with about 12 carbon atoms (three coarse-grained C1 beads in each tail), and systems F−J represent long-chain formulations (16−18 carbons; four C1 beads for each tail).

The simulation systems were built using Packmol[23] and were then run using GROMACS v5.[24,25] The simulation trajectories were visualized using VMD.[26] All simulations used the Martini[12,27] force field v2.2, with polarizable water,[13] using a time step of 20 fs. The energy was first minimized in all systems using steepest descents for 1000 steps followed by an initial equilibration in two stages, first using a 10 fs time step for 300000 steps, and then using a 20 fs time step. Production runs were then carried out for 2 μs for each system separately, again using a 20 fs time step. Pressure and temperature were controlled with the Parinello−Rahman (isotropic) barostat[28] and the velocity rescale thermostat,[29] respectively, and were maintained at 1 bar and 310 K. The relative electrostatic screening was set to 2.5 in accordance with recommendations for polarizable Martini water, with the polarizable water providing explicit screening. Calculations of electrostatics used the reaction-field model, with a cutoff of 1.1 nm, and van der Waals interactions were treated with a plain 1.1 nm cutoff (combined with the potential-shift-Verlet modifier in Gromacs 5).

Data Analysis. The self-mean-square diffusion was calculated using standard Gromacs tools (gmx msd), with the overall center of mass motion removed, and diffusion constants were calculated from the fit to the linear region of these curves.

The cosine similarity is a measure of similarity between two vectors, ranging from −1 to 1. Two vectors with the same orientation have a cosine similarity of 1, two vectors at 90 deg have a similarity of 0, and two opposite vectors have a similarity of −1. We employed this method for the vectors that resulted from monitoring the movement of the head-groups of individual lipids over a period of time (taking vectors from the initial lipid position to the final position). We then calculated the cosine similarity between a central lipid (i.e., the green colored vector in Figure 3) and its immediate neighbors (all black vectors, one-by-one, in Figure 3).

The excess number of "like neighbors" was calculated for a particular lipid as the ratio of the actual number of the same lipid type (tri-, di-, or monoglyceride in this case) within a certain distance and the expected number of lipids of the same type around the central lipid. This latter number was obtained by counting all the lipids in the region and then multiplying by the mole fraction for each lipid type.[30] An excess number larger than 1 indicates that a lipid is more likely to have a like neighbor than an unlike neighbor, suggesting that there is an

DOI: 10.1021/acs.molpharmaceut.7b00397
Mol. Pharmaceutics 2017, 14, 4145−4153

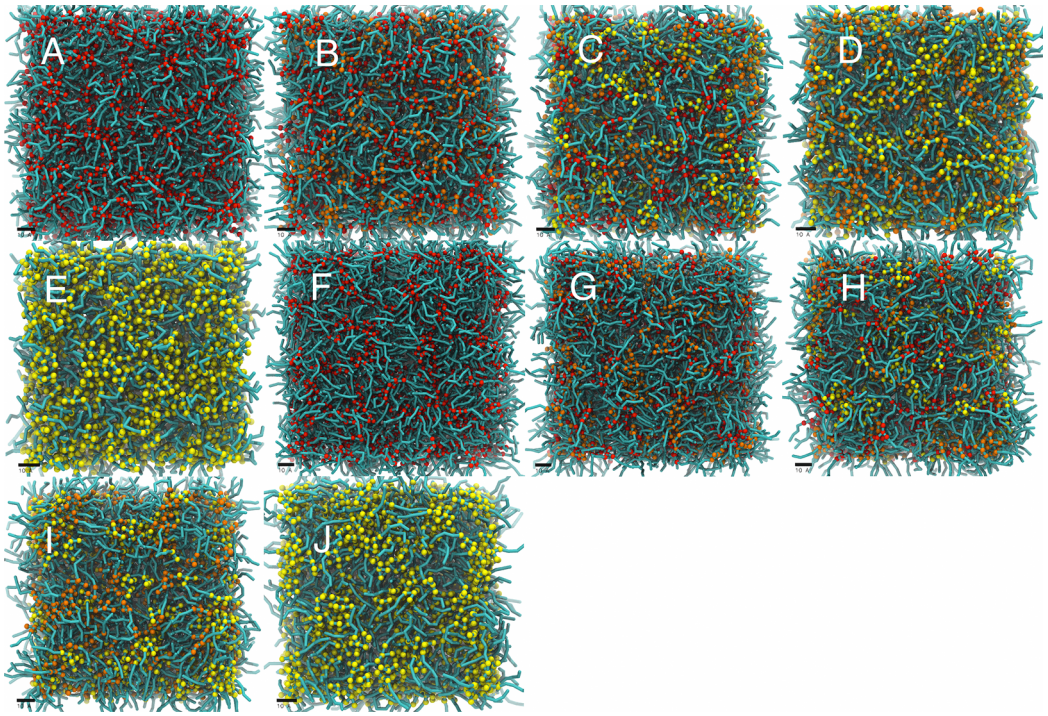

Figure 1. Snapshots of the A–J system configurations with 0% water, after 2 μs. System A is in the top left corner, and system J is in the lower right. Lipid tails are colored cyan, triglyceride head-groups red, diglyceride head-groups orange, and monoglyceride head-groups yellow. For convenience, a scale bar representing 1 nm has been inserted into each snapshot. In these systems, the glycerol head-groups interact with each other, giving rise to nanostructuring resembling inverse micelles. In addition, the head-groups also seem to form long, narrow, worm-like regions.

effective "attraction" between lipids of the same kind or, equivalently, a "repulsion" between lipids of different species.

The second rank order parameter (P2) was calculated from

$$\mathrm{P2} = 0.5 \times (3 \cos^2 \langle\theta\rangle - 1)$$

where θ is the angle between a bond and some normal direction, typically taken to be the bilayer normal (parallel to the z-axis) for bilayer systems, with the angle bracket indicating an ensemble average. P2 = 1 means perfect alignment with the normal, P2 = −0.5 means antialignment, and P2 = 0 means random orientation. Lamellar structures are not always formed with the normal along the z-axis, and, hence, calculations of the P2 order parameter were performed using different normal directions for each case. For simulations with 75% (w/w) water, this direction was identified on a case-by-case basis from the alignments of the lamellar phases in Figure 2, and the same direction was then chosen as the direction for the dry systems as well. The reorientational autocorrelation function $C(t)$ of the P2 order parameter was calculated to further characterize the fluidity of the system in terms of the local dynamic properties. The plateau of $C(t)$ after an extended period corresponds to a residual value and reflects the long-term order of the system.

RESULTS

Phase Behavior. All of the simulated systems spontaneously assembled into different phases, changing with the number of water beads in the system; inverted micellar structures were formed at low water concentrations, and phase-separated, lamellar systems were formed at higher water concentrations, as has previously been observed with AA MD simulations.[8−11] Figures 1 and 2 show the final snapshots (after 2 μs) of all the systems, at 0% and 75% water concentration. For the studied LBFs, phase separation into water- and lipid-rich phases occurred in simulations with water concentrations of 20% to 50%. The analyses we have performed below, as well as visual inspection of the trajectories, do not point to any significant difference between the short (A–E) or long (F–J) lipid chain LBFs with respect to the formation of phases. This is not completely unexpected, and could potentially change with a greater difference in chain length (the lipids simulated herein differed by only one C1 bead in chain length).

Diffusion. As the water content in all the systems was increased from no water to a few, relatively constrained water beads, to almost 45000 Martini water beads (corresponding to 180000 AA water molecules), the self-diffusion of water increased 4-fold, from around 0.5×10^{-5} cm^2/s to approximately 2.0×10^{-5} cm^2/s (Figure S2). This value, for systems with most of the water molecules in the bulk phase, is consistent with both the experimentally reported values for self-diffusion of water (2.3×10^{-5} cm^2/s[12,13,31]) and the polarized Martini water model (2.18×10^{-5} cm^2/s[13]). As previously reported for AA simulations,[8] the situation was markedly different for the lipids. The self-diffusion of the lipids was reduced when the amount of water was increased. Again, this is representative of a phase change; for water concentrations greater than 20%, the lipids form more lamellar phases and therefore are more constrained with regard to motion, and the diffusion coefficient is therefore decreased.

To illustrate in more detail, we monitored the motion of randomly selected lipids and their closest lipid neighbors (within a cutoff distance of 1.0 nm) over a specific time interval. Figure 3 depicts this motion for 0% and 75% water in system A (only medium-chain triglycerides). At the low water concentration (Figure 3a), there are three lipids that are moving in the same direction as the central (green vector) lipid, and five others that move either orthogonally or in the opposite

DOI: 10.1021/acs.molpharmaceut.7b00397
Mol. Pharmaceutics 2017, 14, 4145−4153

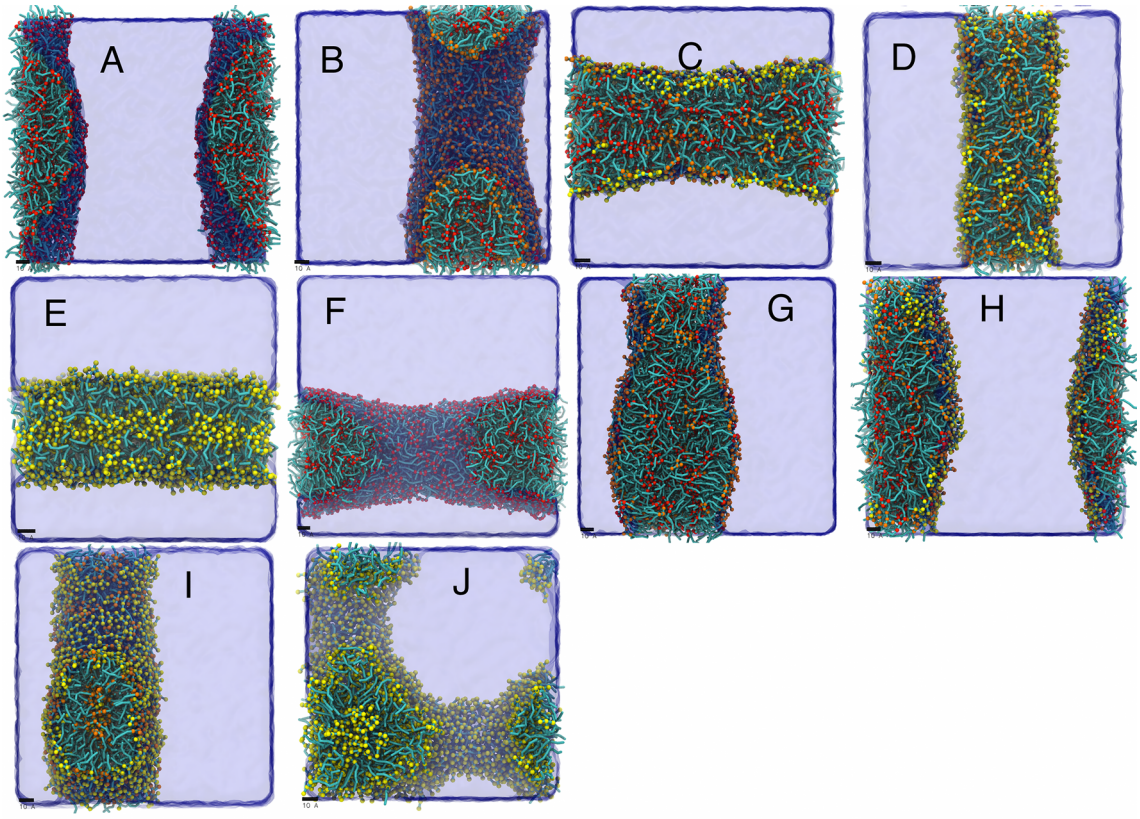

Figure 2. Snapshots of the A−-J system configurations with 75% w/w water concentration, after 2 μs. The color scheme is as in Figure 2, with lipid tails in cyan, triglyceride head-groups in red, diglyceride headgroups in orange, and monoglyceride headgroups in yellow. For convenience, a scale bar representing 1 nm has been inserted into each snapshot. Water particles have been rendered as a transparent surface. Several lamellar phases were formed, and the lipids were partitioned according to kind, with triglycerides (red) moving farthest away from the water, followed by diglycerides, and finally monoglycerides, which were the most common lipids present at the water−lipid boundary.

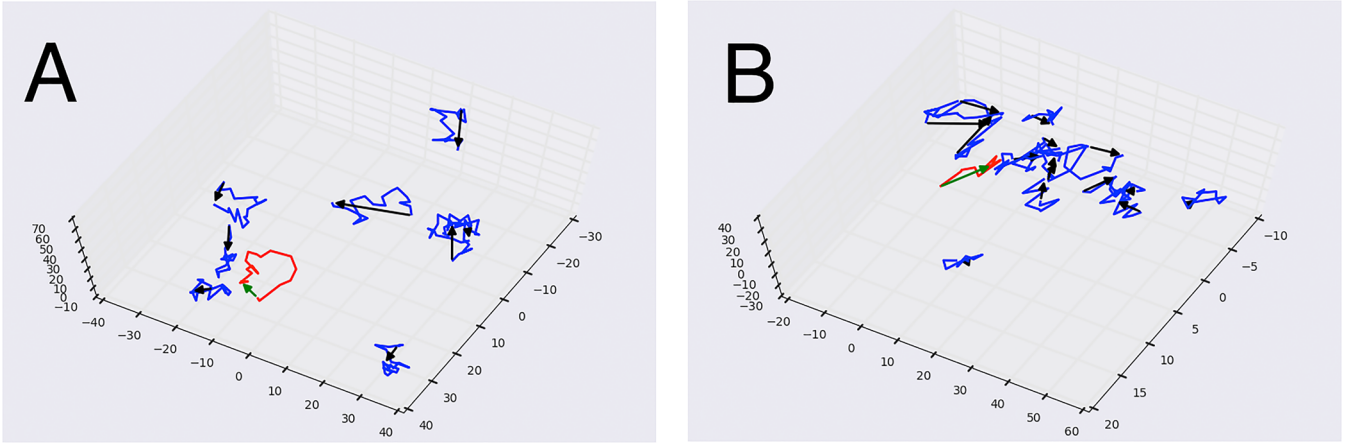

Figure 3. Diffusion of a central lipid (red), and that of its immediate neighbors (blue, within 1 nm cutoff). The plots show (left; no water) a situation where the motion of nearby lipids does not show any particular overall direction, and (right; 75% water) a situation where the orientation of each diffusion vector, on average, is correlated.

direction. As the amount of water was increased, however, the movement patterns of the central lipid became increasingly correlated with those of its neighbors (Figure 3b). We used the cosine similarity to quantify this effect further (Figure 4). For systems with 0% water (and up to 20% water, data not shown), using the cosine similarity, there were no specific correlations between the movements of neighboring lipids. Again, the situation changed when the systems underwent a phase change into a lamellar phase. Figure 4 shows that the frequency of correlated diffusion at 75% water was higher, with more cosine similarities closer to 1, as a consequence of the formation of a lamellar phase, which restricted the movement of individual lipids.

Lipid Packing. Figure 5 shows the radial distribution functions for the lipids in systems C and H (i.e., tri-, di-, and monoglycerides, of medium and long chain lengths, respectively) at 0% and 75% water content. For both systems, at 0% water, there was a sharp peak at about 0.5 nm, followed by a

DOI: 10.1021/acs.molpharmaceut.7b00397
Mol. Pharmaceutics 2017, 14, 4145−4153

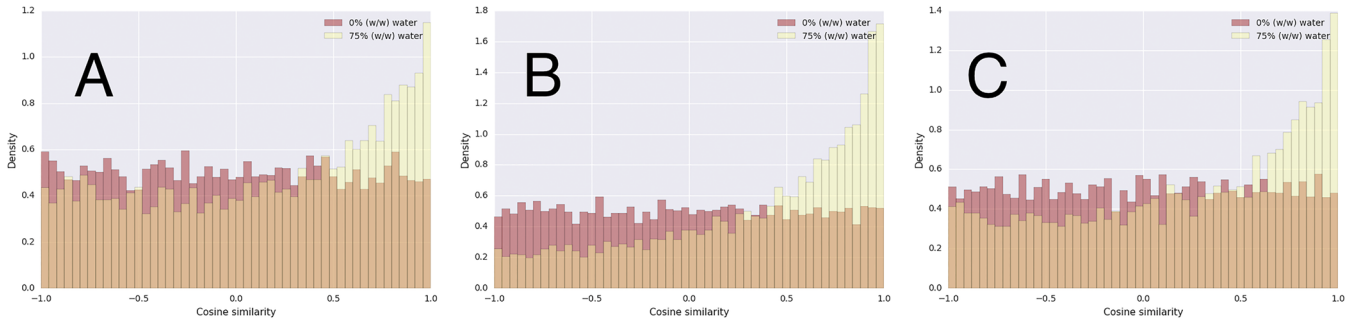

Figure 4. Binned cosine similarities for three systems (systems A, B, and C, see Table 1) at 0% and 75% water concentrations, calculated for the central lipid and its neighbors and averaged over the final 10 frames in each case. Red bars correspond to 0% water, with no overall preference for lipids to move in a correlated fashion, and yellow overlaid bars correspond to the same analysis but for 75% water. There was a clear trend at 75% water for more values closer to 1, which indicates diffusion vectors with the same direction. In particular here, for system B, there was also a decrease in negative values, which further supports the coordinated movement of lipids in systems containing 75% water.

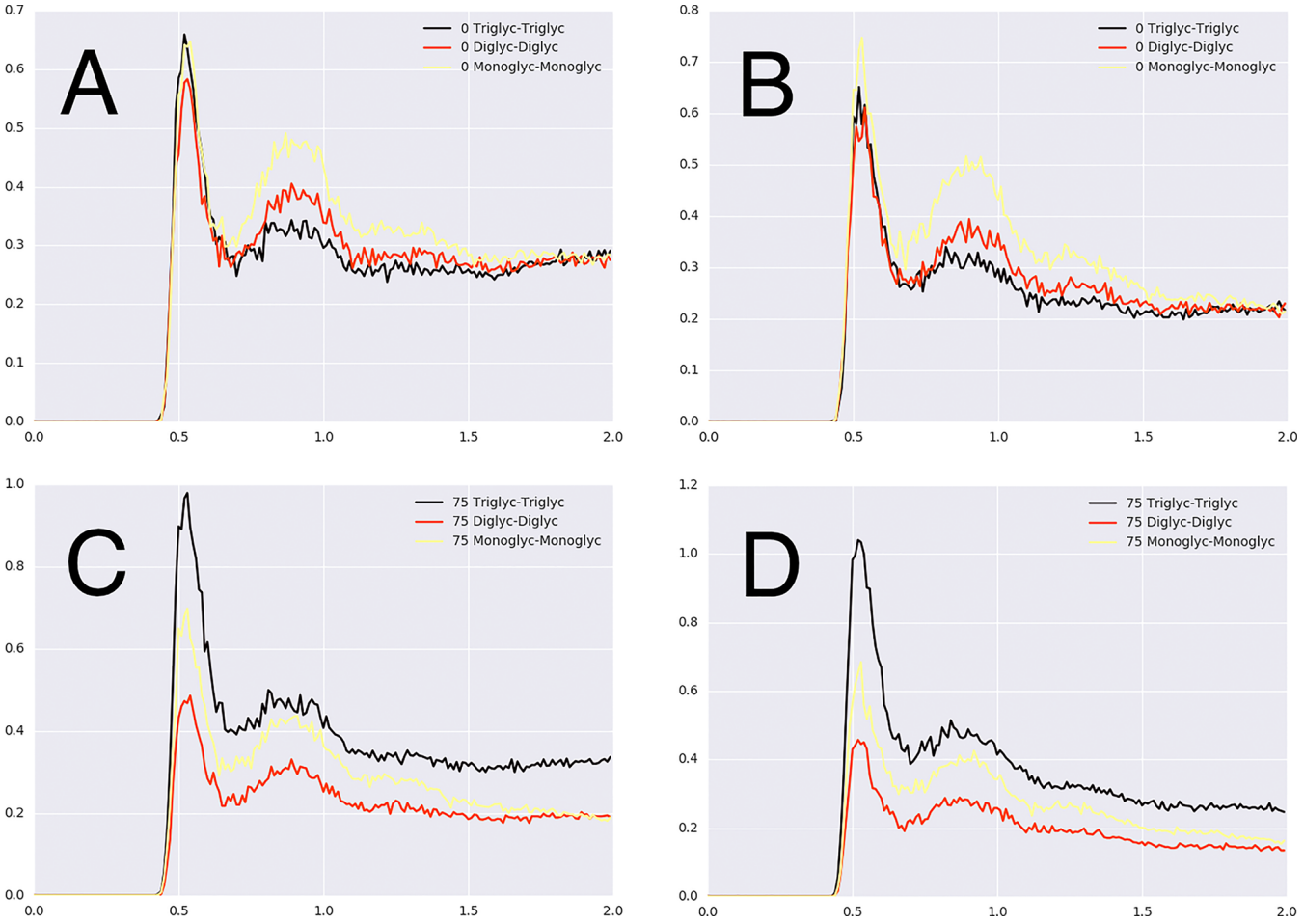

Figure 5. Lipid−lipid radial distribution functions for two systems (system C, panels A and C; and system H, panels B and D) containing all three types of lipids (tri-, di-, and monoglycerides) at 0% (panels A and B) and 75% (panels C and D) water. Distance in nm on *x*-axis, rdf values on *y*-axis.

second peak which was most pronounced for the monoglycerides at 0.7−0.8 nm. There are, however, small, subtle differences between these plots, with the monoglycerides in the long-chain lipid mixtures in particular appearing to associate slightly more closely than either the di- or triglycerides. This may be a result of the ability of the monoglycerides, which have only one lipid tail, to pack more closely together. As the amount of water was increased, these patterns shifted, however, and the relative peak heights of the different lipid types changed. The triglycerides packed most closely in this scenario, presumably as an effect of hydrophobicity, and the energetically more favored system configurations were therefore those that reduced exposure to water. This was also evident from the phases shown in Figure 1 and Figure 2). Interestingly, for both the medium- and long-chain systems (C and H, respectively) at 75% water, the diglyceride peaks were lowest.

Analysis of the distances between the water beads and the lipid head-groups (GLY bead, Figure S3) also provides information on the packing behavior, and the changes that occurred as the amount of water was increased. It was evident

DOI: 10.1021/acs.molpharmaceut.7b00397
Mol. Pharmaceutics 2017, 14, 4145−4153

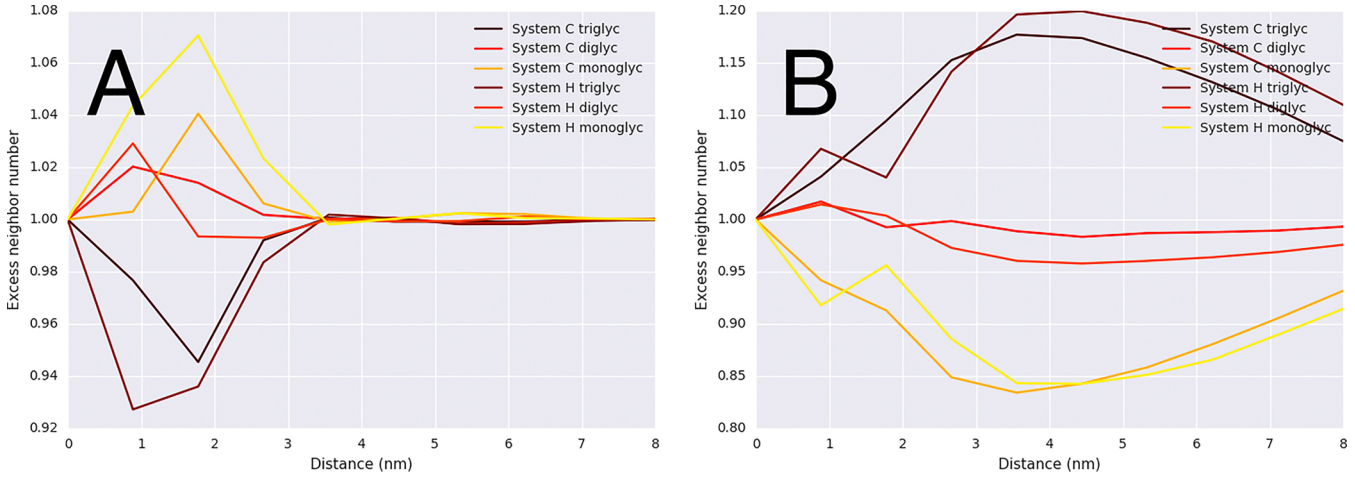

Figure 6. Ratio of the actual number of like neighbors to the expected number of like neighbors for systems C (medium-chain tri-, di-, and monoglycerides) and H (long-chain tri-, di-, and monoglycerides), at 0% (left) and 75% (right) water content. In the dry long-chain system (left panel), there is a relatively higher abundance of monoglycerides near other monoglycerides (1.04 for system C and 1.07 for system H), and there is also a corresponding decrease in the excess number of triglycerides (0.93 and 0.95). The long-term order induced by formation of a lamellar phase at higher water content (right) is also evident.

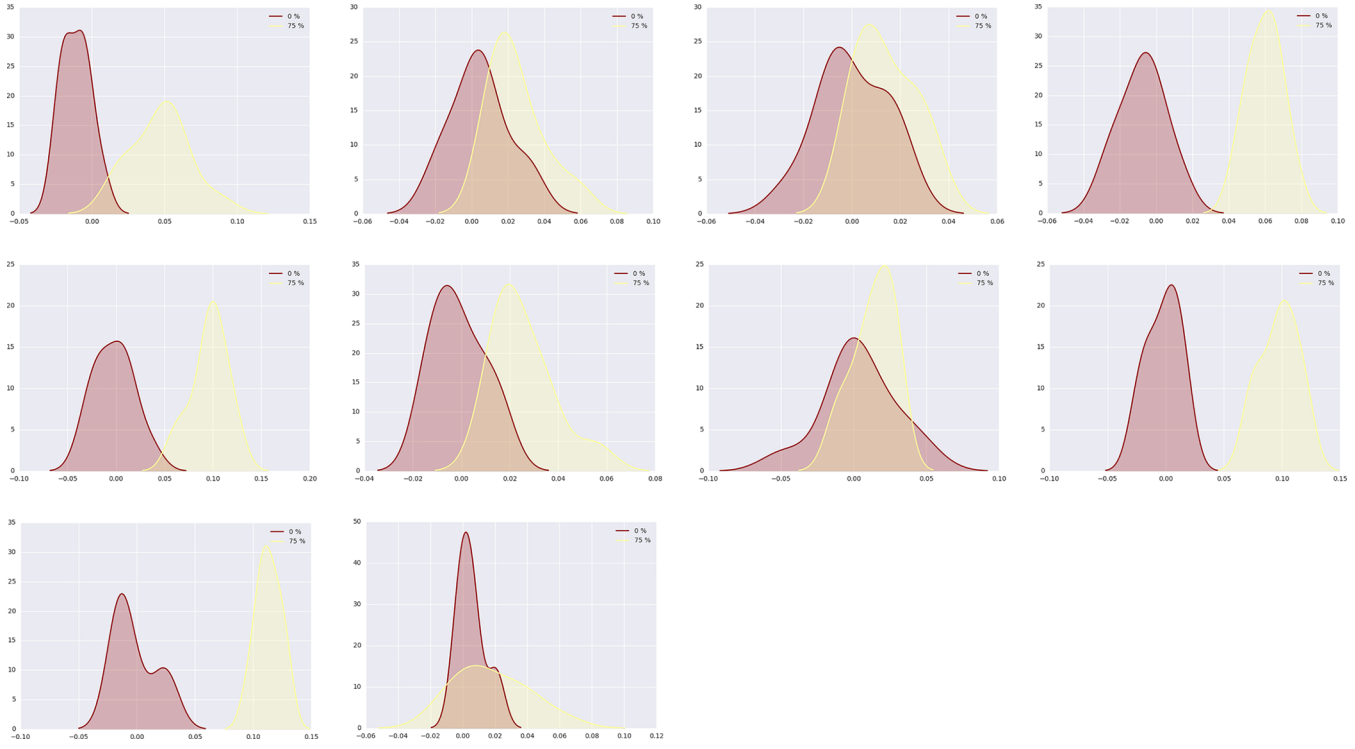

Figure 7. Second rank (P2) order parameters (*x*-axis) shown as histograms (*y*-axis) for all systems A–J (each system in the corresponding figure panel) at 0% (red) and 75% (yellow) water concentration.

that, although the amount of water at low concentrations was not enough to cause complete phase separation, at water concentrations as low as 5% there was a change in how the lipids interacted with water, shown as a distinct peak appearing at approximately 0.5 nm (same as the first maximum in the rdf figures).

Neighboring Like/Unlike Atoms. In a mixture of different kinds of lipids, if the mixture is random, there should be no preference or relative increase in any particular lipid type over any other lipid type. When comparing the two systems that contained tri-, di-, and monoglycerides (systems C and H, with medium- and long-chain lipids, respectively), the monoglycerides were enriched near other monoglycerides (an excess number of 1.04 and 1.07 for C and H), and the triglycerides were similarly depleted near each other (0.95 and 0.93). At longer distances (beyond roughly 3 nm), the dry systems behaved like random mixtures with respect to the different kinds of lipids, whereas formation of lamellar phases meant that the entire box length had to be taken into account before the ratio of like/unlike atoms returns to 1 (Figure 6).

Order Parameters and Reorientational Dynamics. For the majority of the systems, even though the resulting phase with 75% water was not always perfectly lamellar (see, for example, Figure 1, system J), a higher water content induced

DOI: 10.1021/acs.molpharmaceut.7b00397
Mol. Pharmaceutics 2017, 14, 4145–4153

more ordered lipid tails (Figure 7). For some systems (e.g., E) this change was quite significant, and a phase that was almost a double bilayer was formed. General lamellar structures with sometimes very pronounced curvatures were formed for other systems (e.g., systems B and J).

Calculation of the autocorrelation times ($C(t)$) for the P2 order parameter and, in particular, the plateau of $C(t)$ provided information about the long-term, residual order of the systems. Figures S4 and S5 show two major features: (i) the reorientational dynamics of the lipid tails were very rapid in all systems with less than 50% water concentration (only at the higher water concentrations was there any significant long-term order), and (ii) there was no discernible difference in the dynamics between the medium- and long-chain lipid formulations.

DISCUSSION

Lipid molecules are able to self-assemble into a variety of phases with different structures and geometries. The (multifaceted) behavior of lipids in ordered or disordered, crystalline, gel, or liquid-crystalline phases has been studied extensively previously.[32−36] We have focused on the phases formed in various mixtures of tri-, di-, and monoglycerides typically employed in LBFs for poorly soluble drugs, as specified in Table 1, and the dependence of these phases on chain length. We wanted to investigate the degree to which CG MD simulations can be used to study these phenomena. Atomistic systems can be coarse grained on a number of levels, with different consequences. For example, the lack of entropy arising from removing the atomic degrees of freedom (especially from the solvent) can be compensated for with an effective enthalpic term. Temperature-dependent properties should therefore be interpreted with care. CG simulations require much less computational resources than AA simulations and provide faster time-to-solution (the time that is required before converged ensemble properties can be extracted from the simulations). Therefore, if a CG simulation can produce the same phase behavior and partitioning of lipids and water beads as seen with an AA simulation, it will be a very useful computational screening tool for understanding the internal milieu of an LBF, and any subsequent changes to the LBF will obviously affect drug loading and the performance of the LBF in turn.

The phase behavior we have modeled here is consistent with results that have been reported earlier in the literature for AA systems. For example, oleic acid has formed both micellar and lamellar phases at high water concentrations, and oleic acid monoglycerides were locally enriched in a cubic phase when hydrated with 50 to 80% water.[37] Other combinations of lipids and lipid mixtures have also been studied, both experimentally and with computational tools.[38−40] Consistent with the results here, monoolein experimentally forms a lamellar phase at less than 10% water, followed by a cubic phase up to 40% water,[40] and our observation that monoglycerides are enriched in certain phases was also observed previously for oleic acid mixtures.[37] It should be noted in this context that formation of any type of structure in simulations such as these is to some extent dependent on the combination of the size of the box and the number of lipids in the box. The simulation box might be too small for the space required for formation of certain lipid−water phases. Nevertheless, we believe that the simulations represent local environments accurately, i.e., a lipid-rich lamellar phase and bulk water. For example, the presence of high-curvature regions, particularly in the water-rich systems, is in agreement with either of the *Pn*3*m* or *Ia*3*d* cubic phases, and these lipid phases will obviously affect drug solubility and partitioning. The small-scale effects can to some extent be alleviated with a much larger simulation box, and, for example, the recently developed implicit solvent version of the Martini force field[41] (dry Martini) would be interesting to try in this context. As many as six different self-assembled structures of hexagonal, lamellar, and cubic types in the transition from the water-in-oil (w/o) reversed micellar or microemulsion system to an oil-in-water (o/w) micellar or microemulsion system have been reported.[42] Even though the CG mono- and diglycerides used here probably are less surface active than in nature, the fact that we upon dilution see aggregates with triglycerides at the core and mono- and (to a lesser extent) diglycerides forming the surface layer is reassuring, as this has also been observed experimentally.[43]

Diffusion. One of the key characteristics of a system that undergoes a phase change is the change in the self-diffusion of the molecular species that constitute the system. Our results for self-diffusion of water and lipids are in qualitative agreement with those reported earlier.[8] The CG representation introduced by the Martini force field often leads to faster dynamics and a smoother conformational energy landscape,[12] which increases the rate of many processes such as diffusion. While it is difficult to exactly quantify this increase in rate,[12,27] it could explain in part some of the differences in lipid self-diffusion values between our results and those reported earlier. For example, our average diffusion rate for the long-chain systems (F−J) was 0.12×10^{-5} cm^2/s at low water concentrations, reduced to 0.05×10^{-5} cm^2/s at a water concentration of 75%. In comparison, previous values reported from experiments for a monooleate system are 0.018×10^{-5} cm^2/s (approximately 20% water), 0.024×10^{-5} cm^2/s (40% water),[12,44] and 0.02×10^{-5} cm^2/s (81% water).[45]

The longevity of any nanoaggregates formed could also affect drug behavior. Therefore, looking at diffusion as a collective property for a set of neighboring lipids is illuminating. Drugs exhibit very different solubility and partitioning profiles when the local environment around them changes. To this end, we have tried to quantify the degree to which aggregates move in concert, similarly to what has been done for all-atom simulations before,[30,46] that is, whether lipids that are near to each other stay with the same surrounding lipids over time. This was done as a means of exploring the stability of the various kinds of aggregates that are formed in lipid mixtures, in order to provide insight into any rearrangements that might be occurring, particularly in the dry systems. We found evidence for diffusion behavior changing as the amount of water in the system changes. For a completely dry system, over the time scales we analyzed (200 ns), any local microstructure existed only transiently, as judged by calculating the distribution of cosine similarities, whereas higher water concentrations led to formation of local environments that did not change as much (Figures 3 and 4).

Neighboring Like/Unlike Atoms. Experimental determination of the local distribution of lipids is challenging, even for better-defined systems such as bilayers. In a random mixture, the mean composition of all neighboring lipids in a sufficiently large circle drawn around a lipid of either type will be the same and will reflect the bulk composition. It should be noted that this may not be true at short distances, because molecular sizes or shapes may lead to different distributions of neighbor

DOI: 10.1021/acs.molpharmaceut.7b00397
Mol. Pharmaceutics 2017, 14, 4145−4153

distances for different types of neighbors, even if the overall distribution is random. We noted subtle differences between medium- and long-chain lipid systems (Figure 6). In the dry systems, the monoglycerides had a positive excess of like neighbors (up to 1.07 for the monoglycerides in system H and 1.04 for system C when measured as described elsewhere), whereas the triglycerides had negative excess at short distances (0.93 and 0.95, up to a distance of 3 nm). This correlated quantitatively with the radial distribution functions for systems C and H (Figure 5, A and B) without water, where the monoglycerides appeared to form a well-defined second solvation shell out to a distance of about 1.5 nm. Although the long distance analysis of these systems points at a random mixture of excipients, the short distance (few nanometers) points at local small clusters of the components that are not mixed to any larger extent with the other excipients. This may explain, at least in part, the additive solubility effect of the excipients included in an LBF that has been observed experimentally.[20] The simulations indicate that each of the included excipients forms local nanostructures in the dry LBF and that the interaction between the excipients is minimal. Hence, based on the results from the simulations, we speculate that, when drug molecules dissolve in the LBF, they simply saturate each of the included components. The total loading capacity of the formulation therefore equals the sum of the concentrations possible to dissolve in each excipient volume fraction.

Orientational Dynamics. By calculating the second rank order parameter along the entire lipid tail (as opposed to calculating for each bond separately), we have shown that all systems underwent a change from a state in which the lipid tails had no preferred direction (order parameters around 0, Figure 7) to a relatively more ordered configuration (histogram peaks moving toward positive P2 values) when the water content was increased. The lack of overall order in the dry systems does not mean that there was no local structuring, which, as stated above, indeed does exist. We emphasize here that calculations of order parameters have typically been carried out for (preformed) lipid bilayers, where their interpretation is more straightforward. Here, matters were more complicated, since not all systems form bilayered phases with a well-defined normal direction. Also the presence of high-curvature regions (for example, system J) means that the use of a fixed director axis for the order parameter calculation likely "hides" some of the ordering that is observed visually.

Calculations of P2 autocorrelations (Figures S4 and S5) showed that the lipids are able to maintain their relative orientation with respect to some director only at high water concentrations, which is consistent with the correlated diffusion behavior found for nearby lipids in water concentrations above 50%. This further supports our observation that the local nanostructuring that does occur in dry systems is of a transient nature.

CONCLUSIONS

Coarse grained molecular dynamics simulation is a step toward virtual screening of nanostructures and phase transition of lipid-based drug delivery systems. For the systems studied herein we observed nanostructures of lipids, that are dynamic in composition and over time, in the dry formulation. These structures provide an explanation to previous experimental data on drug loading capacity of LBFs. As the amount of water is increased, the simulation systems undergo a phase transition into separate lipid and water phases. At a water content mimicking a dispersed lipid-filled capsule after intake with a glass of water, these lipid phases are ordered on several levels. In contrast to AA simulations, coarse-graining has the advantage that it drastically reduces computation times and enables studies of drug disposition, partitioning, and solubility at relevant physiological conditions since larger box sizes can be explored. Hence, we view CG molecular dynamics as a way forward to computationally screen molecular interactions between water, drug molecules, and components of complex formulations such as LBFs.

ASSOCIATED CONTENT

Supporting Information

The Supporting Information is available free of charge on the ACS Publications website at DOI: 10.1021/acs.molpharmaceut.7b00397.

CG molecular structures, self-diffusion coefficients vs water concentration, lipid−water distances, and P2 autocorrelations (PDF)

AUTHOR INFORMATION

Corresponding Author

*E-mail: larsson.r.per@gmail.com.

ORCID

Per Larsson: 0000-0002-8418-4956

Notes

The authors declare no competing financial interest.

ACKNOWLEDGMENTS

This work has received support from the Innovative Medicines Initiative Joint Undertaking (http://www.imi.europa.eu) under Grant Agreement No. 115369, resources of which are composed of financial contributions from the European Union's Seventh Framework Programme (FP7/2007-2013) and EFPIA companies. Financial support was also received from the European Research Council Grant 638965 and the Swedish Research Council Grant 2014-3309. The simulations were performed on resources provided by the Swedish National Infrastructure for Computing (SNIC) at the PDC Centre for High Performance Computing (PDC-HPC), the National Supercomputer Center (NSC), and the High Performance Computing Center North (HPC2N).

REFERENCES

(1) Pouton, C. W. *Eur. J. Pharm. Sci.* **2006**, *29* (3-4), 278.
(2) Patel, S. V.; Patel, S. *Eur. J. Pharm. Sci.* **2015**, *77*, 161.
(3) Starov, V. M., Ed. *Nanoscience: colloidal and interfacial aspects*; CRC Press: Boca Raton, FL, 2010.
(4) Rajabalaya, R.; Musa, M. N.; Kifli, N.; David, S. R. *Drug Des., Dev. Ther.* **2017**, *11*, 393.
(5) Weerapol, Y.; Kumpugdee-Vollrath, M.; Sriamornsak, P. *Adv. Mater. Res.* **2013**, *747*, 139.
(6) Pasenkiewicz-Gierula, M.; Takaoka, Y.; Miyagawa, H.; Kitamura, K.; Kusumi, A. *J. Phys. Chem. A* **1997**, *101*, 3677.
(7) Róg, T.; Murzyn, K.; Pasenkiewicz-Gierula, M. *Chem. Phys. Lett.* **2002**, *352*, 323.
(8) Warren, D. B.; King, D.; Benameur, H.; Pouton, C. W.; Chalmers, D. K. *Pharm. Res.* **2013**, *30* (12), 3238.
(9) Birru, W. A.; Warren, D. B.; Headey, S. J.; Benameur, H.; Porter, C. J. H.; Pouton, C. W.; Chalmers, D. K. *Mol. Pharmaceutics* **2017**, *14* (3), 566.

DOI: 10.1021/acs.molpharmaceut.7b00397
Mol. Pharmaceutics 2017, 14, 4145−4153

(10) Birru, W. A.; Warren, D. B.; Han, S.; Benameur, H.; Porter, C. J. H.; Pouton, C. W.; Chalmers, D. K. *Mol. Pharmaceutics* **2017**, *14* (3), 580.
(11) Ingólfsson, H. I.; Lopez, C. A.; Uusitalo, J. J. *WIREs Comput. Mol. Sci* **2014**, *4*, 225.
(12) Monticelli, L.; Kandasamy, S. K.; Periole, X.; Larson, R. G.; Tieleman, D. P.; Marrink, S.-J. *J. Chem. Theory Comput.* **2008**, *4* (5), 819.
(13) Yesylevskyy, S. O.; Schäfer, L. V.; Sengupta, D.; Marrink, S. J. *PLoS Comput. Biol.* **2010**, *6* (6), e1000810.
(14) Edholm, O.; Tjörnhammar, R.; Waheed, Q. *Biophys. J.* **2013**, *104* (2), 590a.
(15) Rodgers, J. M.; Sørensen, J.; de Meyer, F. J. M.; Schiøtt, B.; Smit, B. *J. Phys. Chem. B* **2012**, *116* (5), 1551.
(16) Dahlberg, M. *J. Phys. Chem. B* **2007**, *111* (25), 7194.
(17) Fuhrmans, M.; Marrink, S. J. *J. Am. Chem. Soc.* **2012**, *134* (3), 1543.
(18) Marrink, S. J.; Tieleman, D. P. *Chem. Soc. Rev.* **2013**, *42* (16), 6801.
(19) Sacchetti, M.; Nejati, E. *AAPS PharmSciTech* **2012**, *13* (4), 1103.
(20) Alskär, L. C.; Bergström, C. *Curr. Mol. Biol. Rep.* **2015**.
(21) Alskär, L. C.; Porter, C. J. H.; Bergström, C. A. S. *Mol. Pharmaceutics* **2016**, *13* (1), 251.
(22) Vuorela, T.; Catte, A.; Niemelä, P. S.; Hall, A.; Hyvönen, M. T.; Marrink, S.-J.; Karttunen, M.; Vattulainen, I. *PLoS Comput. Biol.* **2010**, *6* (10), e1000964.
(23) Martínez, L.; Andrade, R.; Birgin, E. G.; Martínez, J. M. *J. Comput. Chem.* **2009**, *30* (13), 2157.
(24) Pronk, S.; Páll, S.; Schulz, R.; Larsson, P.; Bjelkmar, P.; Apostolov, R.; Shirts, M. R.; Smith, J. C.; Kasson, P. M.; van der Spoel, D.; Hess, B.; Lindahl, E. *Bioinformatics* **2013**, *29*, 845.
(25) Abraham, M. J.; Murtola, T.; Schulz, R.; Páll, S.; Smith, J. C.; Hess, B.; Lindahl, E. *SoftwareX* **2015**, *1*−*2*, 19.
(26) Humphrey, W.; Dalke, A.; Schulten, K. *J. Mol. Graphics* **1996**, *14* (1), 33.
(27) Marrink, S. J.; Risselada, H. J.; Yefimov, S.; Tieleman, D. P.; de Vries, A. H. *J. Phys. Chem. B* **2007**, *111* (27), 7812.
(28) Parrinello, M.; Rahman, A. *J. Appl. Phys.* **1981**, *52* (12), 7182.
(29) Bussi, G.; Donadio, D.; Parrinello, M. *J. Chem. Phys.* **2007**, *126* (1), 014101.
(30) Coppock, P. S.; Kindt, J. T. *Langmuir* **2009**, *25* (1), 352.
(31) Holz, M.; Heil, S. R.; Sacco, A. *Phys. Chem. Chem. Phys.* **2000**, *2* (20), 4740.
(32) Tardieu, A.; Luzzati, V.; Reman, F. C. *J. Mol. Biol.* **1973**, *75* (4), 711.
(33) Chapman, D. *Q. Rev. Biophys.* **1975**, *8* (2), 185.
(34) Koynova, R.; Tenchov, B. *OA Biochem.* **2013**, DOI: 10.13172/2052-9651-1-1-602.
(35) Demurtas, D.; Guichard, P.; Martiel, I.; Mezzenga, R.; Hébert, C.; Sagalowicz, L. *Nat. Commun.* **2015**, *6*, 8915.
(36) Tate, M. W.; Eikenberry, E. F.; Turner, D. C. *Chem. Phys. Lipids* **1991**, *57* (2-3), 147.
(37) Pitzalis, P.; Monduzzi, M.; Krog, N.; Larsson, H.; Ljusberg-Wahren, H.; Nylander, T. *Langmuir* **2000**, *16* (15), 6358.
(38) Larsson, K.; Krog, N. *Chem. Phys. Lipids* **1973**, *10* (2), 177.
(39) Janke, J. J.; Bennett, W. F. D.; Tieleman, D. P. *Langmuir* **2014**, *30* (35), 10661.
(40) Borné, J.; Nylander, T.; Khan, A. *Langmuir* **2001**, *17* (25), 7742.
(41) Arnarez, C.; Uusitalo, J. J.; Masman, M. F.; Ingólfsson, H. I.; de Jong, D. H.; Melo, M. N.; Periole, X.; de Vries, A. H.; Marrink, S. J. *J. Chem. Theory Comput.* **2015**, *11* (1), 260.
(42) Sagalowicz, L.; Leser, M. E.; Watzke, H. J. *Trends Food Sci. Technol.* **2006**, *17* (5), 204.
(43) Prajapati, H. N.; Dalrymple, D. M.; Serajuddin, A. T. M. *Pharm. Res.* **2012**, *29* (1), 285.
(44) Eriksson, P. O.; Lindblom, G. *Biophys. J.* **1993**, *64* (1), 129.
(45) Geil, B.; Feiweier, T.; Pospiech, E. M.; Eisenblätter, J.; Fujara, F.; Winter, R. *Chem. Phys. Lipids* **2000**, *106* (2), 115.
(46) Falck, E.; Róg, T.; Karttunen, M.; Vattulainen, I. *J. Am. Chem. Soc.* **2008**, *130* (1), 44.

DOI: 10.1021/acs.molpharmaceut.7b00397
Mol. Pharmaceutics 2017, 14, 4145−4153